Optical−Optical Double Resonance Spectroscopy of the $C^2\Pi-A^2\Pi$ and $D^2\Sigma^+-A^2\Pi$ Transitions of SrF†

Phillip M. Sheridan,[‡,§] Jin-Guo Wang,[‡,||] Michael J. Dick,[⊥,#] and Peter F. Bernath*[,‡,||]

Department of Chemistry and Department of Physics, University of Waterloo, Waterloo, Ontario N2L 3G1, Canada

Received: March 8, 2009; Revised Manuscript Received: April 7, 2009

Optical−optical double resonance spectroscopy has been used to record rotationally resolved spectra of the $C^2\Pi-A^2\Pi$ and $D^2\Sigma^+-A^2\Pi$ transitions of SrF. In the investigation, the spectrum of a previously unobserved $^2\Sigma^+-A^2\Pi$ transition was recorded. The new $^2\Sigma^+$ state was found to lie lower in energy than the previously labeled $D^2\Sigma^+$ ($v = 0$) state by an amount equal to the vibrational spacing of the $D^2\Sigma^+$ state. Therefore, the new $^2\Sigma^+$ state was assigned as the $v = 0$ level of the $D^2\Sigma^+$ state and the previous labeling of the vibrational quantum numbers of the $D^2\Sigma^+$ state should be increased by 1. Spectroscopic parameters were determined for the $C^2\Pi$, $D^2\Sigma^+$ ($v = 0$), and $D^2\Sigma^+$ ($v = 1$) states. The $D^2\Sigma^+$ ($v = 0$) state was found to be perturbed, most likely by the spin−orbit components of the $C^2\Pi$ ($v = 1$) state. The spin−orbit constant of the $C^2\Pi$ state was found to decrease significantly relative to the $A^2\Pi$ state, similar to CaF and SrOH. Finally, the $C^2\Pi$ and $D^2\Sigma^+$ states do not appear to form a unique perturber/pure precession pair of states.

1. Introduction

Of all the alkaline-earth metal containing radicals, CaF has been investigated the most extensively. The electronic states of CaF with energies less than 35000 cm^{-1} have been well-characterized by a variety of spectroscopic studies[1−6] and the higher energy Rydberg states have also been investigated.[7−9] The Field group has not only pioneered many of these spectroscopic studies but also provided a detailed understanding of the electronic structure of CaF.[10−14] SrF, on the other hand, which has an electronic structure similar to that of CaF and could serve as a useful comparison, has not been investigated to the same degree. Recently there has been a renewed interest in these molecules, because of their potential to measure nuclear spin dependent parity violation.[15]

Some of the earliest analyses of the band spectra of SrF were completed by Johnson in 1929[16] and Harvey in 1931.[17] In 1941 Fowler[18] reported four new electronic bands of SrF, expanding the number of known electronic states below 35000 cm^{-1} to eight. For each of these states, term values and vibrational frequencies were reported. Since then the lower energy states of SrF have been the subject of numerous spectroscopic investigations. In the 1970s laser excitation spectroscopy was used to obtain rotationally resolved spectra of the $A^2\Pi-X^2\Sigma^+$ [10] and the $B^2\Sigma^+-X^2\Sigma^+$ [20] transitions. More recently, molecular beam techniques have been used to further investigate the $A^2\Pi-X^2\Sigma^+$ transition[21] and intermodulated fluorescence spectroscopy and Doppler free polarization spectroscopy have been used to expand the study of the $B^2\Sigma^+-X^2\Sigma^+$ transition.[22,23] In addition, millimeter-wave spectroscopy and double resonance techniques have been used to ascertain the rotational, fine structure, and hyperfine parameters of the $X^2\Sigma^+$ state.[24−28] A high-resolution infrared emission spectrum of SrF has been recorded, and Dunham parameters for the ground $X^2\Sigma^+$ state have been reported.[29] Finally, the permanent electric dipole moment of SrF in the $X^2\Sigma^+$, $A^2\Pi$, and $B^2\Sigma^+$ electronic states has been measured.[30,31]

The higher energy states of SrF, on the other hand, have not received nearly as much attention. Barrow and Beale[32] reported a rotational analysis of the $F^2\Sigma^+-X^2\Sigma^+$ transition in 1967. Subsequently, optical−optical double resonance (OODR) spectroscopy was used to investigate the $F^2\Sigma^+-B^2\Sigma^+$ and $G^2\Pi-B^2\Sigma^+$ transitions.[33] In the OODR study, rotational and fine structure constants were reported for both the $F^2\Sigma^+$ and $G^2\Pi$ states. The $C^2\Pi-X^2\Sigma^+$ transition was examined at higher resolution using emission spectroscopy by Novikov and Gurvich[34] in 1967. Their work resulted in an improved vibrational analysis of the $C^2\Pi$ state. Two additional investigations of the $C^2\Pi-X^2\Sigma^+$ transition further refined the vibrational analysis of the $C^2\Pi$ state and reported the first estimate of the rotational constant.[35,36] Both the $E^2\Pi$ and $D^2\Sigma^+$ states have not been the subject of any high-resolution spectroscopic work, and the lowest $^2\Delta$ state has yet to be observed.

One of the reasons that the higher energy states (>20000 cm^{-1}) of SrF have not yet been investigated by high-resolution laser spectroscopy is the difficulty in accessing these states. OODR spectroscopy has been used successfully to investigate higher energy states; however, the technique has generally involved the use of two single mode lasers, which makes the recording of spectra a tedious process. Recently, we have determined spectroscopic parameters for the $\tilde{B}'^2\Sigma^+$, $\tilde{C}^2\Pi$, and $\tilde{D}^2\Sigma^+$ states of SrOH, the $\tilde{C}^2\Pi$ state of SrOD, and the $\tilde{D}^2\Sigma^+$ state of CaOH using a modified version of this technique.[37−40] In our studies a broad-band laser was used as the pump laser for the first transition in order to maximize the number of rotational levels populated in the intermediate state. While this resulted in congested spectra, the tediousness associated with

† Part of the "Robert W. Field" Festschrift.

* Corresponding author: e-mail, pfb500@york.ac.uk; tel, +44-1904-434526; fax, +44-1904-432516.

‡ Department of Chemistry, University of Waterloo.

§ Current address: Department of Chemistry and Biochemistry, Canisius College, Buffalo, NY 14208.

|| Current address: Department of Chemistry, University of York, Heslington, York, YO10 5DD, U.K.

⊥ Department of Physics, University of Waterloo.

Current address: Jet Propulsion Laboratory, California Institute of Technology, 4800 Oak Grove Dr., Pasadena, CA, 91109-9099.

10.1021/jp9020855 CCC: $40.75
Published on Web 05/04/2009

the recording of the spectra was removed. We decided to further utilize this technique to investigate the $C^2\Pi$ and $D^2\Sigma^+$ states of SrF in order to better understand its electronic structure and to allow for a comparison of the spectroscopic parameters with the corresponding states in CaF and SrOH.

In this paper we present the results of our investigation of the $C^2\Pi$ and $D^2\Sigma^+$ states of SrF. Spectra of the $C^2\Pi-A^2\Pi$ and $D^2\Sigma^+-A^2\Pi$ transitions were recorded using OODR spectroscopy, and spectroscopic parameters were determined for the $C^2\Pi$ and $D^2\Sigma^+$ states. In our investigation, a new $^2\Sigma^+-A^2\Pi$ transition was discovered at a lower energy than the $D^2\Sigma^+-A^2\Pi$ transition. The new $^2\Sigma^+$ state was found to lie lower in energy than the $D^2\Sigma^+$ state by an amount equal to the vibrational spacing of the $D^2\Sigma^+$ state. This suggested that the new $^2\Sigma^+$ state was actually the $v = 0$ level of the $D^2\Sigma^+$ state and that the previous numbering of the vibrational levels of the $D^2\Sigma^+$ state should be increased by 1, similar to the situation encountered for the $D^2\Sigma^+$ state of CaF.[2,6] Although the $D^2\Sigma^+$ ($v = 0$) state was found to be perturbed, a limited rotational analysis supports this assignment. A discussion of the evidence for renumbering the vibrational levels of the $D^2\Sigma^+$ state, the nature of the perturbation in the $D^2\Sigma^+$ ($v = 0$) state, an analysis of the spectroscopic parameters in the $C^2\Pi$ and $D^2\Sigma^+$ states of SrF, and a comparison of these parameters to those in the equivalent states of CaF and SrOH follows.

2. Experimental Section

The synthesis of strontium monofluoride was similar to the method previously described in detail in our OODR study of SrOH.[7] Briefly, strontium vapor was produced by resistively heating a graphite crucible containing strontium metal in a Broida-type oven. The metal vapor was then directed into a reaction region above the oven using a flow of argon gas. In the reaction region approximately 10 mTorr of SF_6 gas was introduced to produce SrF. A bright chemiluminescent flame was observed when SrF production was optimal.

OODR spectroscopy was used to record high-resolution spectra of the (0,0) $C^2\Pi_{1/2}-A^2\Pi_{1/2}$, (0,0) $C^2\Pi_{3/2}-A^2\Pi_{3/2}$, (1,0) $D^2\Sigma^+-A^2\Pi_{1/2}$, (1,0) $D^2\Sigma^+-A^2\Pi_{3/2}$, (0,0) $D^2\Sigma^+-A^2\Pi_{1/2}$, and (0,0) $D^2\Sigma^+-A^2\Pi_{3/2}$ transitions of SrF. To do this, band heads of either the (0,0) $A^2\Pi_{1/2}-X^2\Sigma^+$ or (0,0) $A^2\Pi_{3/2}-X^2\Sigma^+$ transition were first excited using a linear cavity dye (pump) laser (~1 cm^{-1} bandwidth, DCM laser dye). A Burleigh WA-2500 Wavemeter Jr. was used to monitor the frequency of the pump laser. Subsequently, SrF molecules that had been promoted to the intermediate $A^2\Pi_{1/2}$ or $A^2\Pi_{3/2}$ spin−orbit states were probed with a single-mode Coherent 899 Ti-sapphire (probe) laser (~10 MHz bandwidth). While the probe laser was scanned, the frequency of the pump laser remained fixed. When the frequency of the probe laser corresponded to a resonance between a rotational level of one of the spin−orbit components of the $A^2\Pi$ state and a rotational level of an excited electronic state ($C^2\Pi$ or $D^2\Sigma^+$), the resulting UV fluorescence was observed using a photomultiplier tube (PMT). To significantly reduce scattered light from the pump laser and fluorescence from the $A^2\Pi$ state from reaching the PMT, a 500 nm blue pass filter was utilized. To further ensure that the signals observed in this experiment were due to the OODR excitation, phase sensitive detection was utilized by mechanically chopping the pump beam and processing the modulated fluorescence signal from the PMT using a lock-in amplifier. Spectra were obtained in 5 cm^{-1} segments at a scan speed of 2 GHz per second and a data sampling interval of 20 MHz. The absorption spectrum of heated I_2 was recorded simultaneously to determine the absolute frequency of the probe laser. The 6 GHz Fabry−Perot fringes from the Coherent 899-29 wavemeter were monitored to ensure continuity of the probe laser scan.

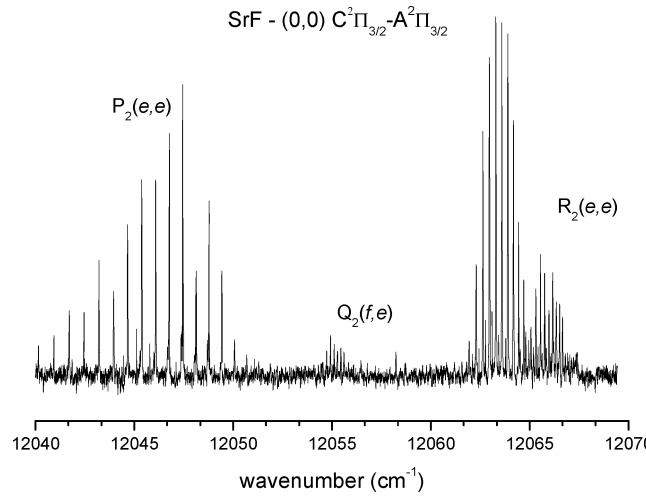

Figure 1. Rotationally resolved spectrum of the (0,0) $C^2\Pi_{3/2}-A^2\Pi_{3/2}$ transition of SrF. The lines in the spectrum were assigned to three branches, which exhibit the characteristic appearance of a Hund's case (a) $^2\Pi$−Hund's case (a) $^2\Pi$ transition. Due to the rotational energy levels populated in the $A^2\Pi_{3/2}$ state having predominately e parity and low probe laser power in this region, transitions arising from the P_2(ff), R_2(ff), and Q_2(ef) branches were not observed.

3. Results

To begin the investigation of the $C^2\Pi-A^2\Pi$ transition an approximate frequency range for the probe laser was calculated using the previously reported[18] term value for the $C^2\Pi$ state of SrF. Initially, the pump laser was tuned to 15070 cm^{-1}, which excited the band heads of the Q_{12}(ef) and P_{11}(ee) branches of the (0,0) $A^2\Pi_{1/2}-X^2\Sigma^+$ transition of SrF. A high-resolution spectrum of the (0,0) $C^2\Pi_{1/2}-A^2\Pi_{1/2}$ transition was obtained by scanning the probe laser in the 12210−12300 cm^{-1} range. A large number of spectral features were observed because of the many rotational levels populated in the $A^2\Pi_{1/2}$ state as a result of the 1 cm^{-1} bandwidth of the pump laser and energy transfer due to collisions. The spectrum was found to exhibit the branch structure characteristic of a Hund's case (a) $^2\Pi$−Hund's case (a) $^2\Pi$ transition. With lower state combination differences, rotational quantum numbers were assigned to each spectral feature. Transitions in the R_1(ee), P_1(ee), and Q_1(fe) branches were the most intense due to the populated rotational energy levels of the $A^2\Pi_{1/2}$ state being predominately e-parity. Transitions belonging to branches with a lower state rotational energy level of f-parity, R_1(ff) and P_1(ff), were found to be less intense. No transitions belonging to the Q_1(ef) branch were observed. Subsequently, the band heads of the Q_{22}(ef) and P_{21}(ee) branches of the (0,0) $A^2\Pi_{3/2}-X^2\Sigma^+$ transition were excited by the pump laser (15352 cm^{-1}) in order to observe the (0,0) $C^2\Pi_{3/2}-A^2\Pi_{3/2}$ transition. The probe laser was scanned in the range of 12040−12070 cm^{-1} and a rotationally resolved spectrum of the (0,0) $C^2\Pi_{3/2}-A^2\Pi_{3/2}$ transition was recorded and is shown in Figure 1. Again lower state combination differences were used to assign quantum numbers to the lines. In Figure 1 transitions in the P_2(ee) branch are found on the lower wavenumber side and transitions in the R_2(ee) branch are present on the higher wavenumber side. Between these two branches, a few weaker features arising from the Q_2(fe) branch are shown. This spectrum has the characteristic appearance of a Hund's case (a) $^2\Pi$−Hund's case (a) $^2\Pi$ transition. Due to

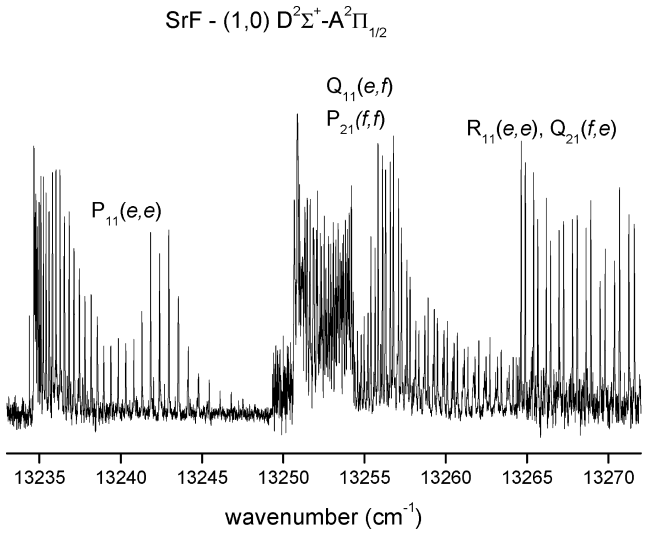

Figure 2. The spectrum of the (1,0) $D^2\Sigma^+-A^2\Pi_{1/2}$ transition. The appearance of the spectrum is typical of a Hund's case (b) $^2\Sigma$ Hund's case (a) $^2\Pi$ transition. Lines belonging to five (P_{11}, P_{21}, Q_{11}, Q_{21}, and R_{11}) of the six possible branches were identified. Band heads were observed in the P_{11}, P_{21}, and Q_{11} branches.

the rotational energy levels populated in the $A^2\Pi_{3/2}$ state having predominately e parity and low probe laser power in this region, transitions arising from the P_2(ff), R_2(ff), and Q_2(ef) branches were not observed.

The $D^2\Sigma^+-A^2\Pi$ transition was investigated using the previous work of Fowler to calculate a frequency range to scan the probe laser.[18] Again, a pump laser frequency of 15070 cm^{-1} was used to excite the Q_{12} and P_{11} band heads of the (0,0) $A^2\Pi_{1/2}-X^2\Sigma^+$ transition. The probe laser was scanned from 13230 to 13285 cm^{-1} and the majority of the measured spectrum of the $D^2\Sigma^+-A^2\Pi_{1/2}$ transition is shown in Figure 2. The spectrum has the appearance of a Hund's case (b) $^2\Sigma-$Hund's case (a) $^2\Pi$ transition. Quantum numbers were assigned to the spectral features using lower state combination differences, and transitions belonging to the P_{11}, P_{21}, Q_{11}, Q_{21}, and R_{11} branches were identified. From this spectrum a refined term value for the $D^2\Sigma^+$ state was calculated and the pump laser frequency was then shifted to 15352 cm^{-1} to excite the band heads of the Q_{22} and P_{21} branches of the (0,0) $A^2\Pi_{3/2}-X^2\Sigma^+$ transition. A spectrum of the $D^2\Sigma^+-A^2\Pi_{3/2}$ transition was then obtained by scanning the probe laser in the range 12950−13010 cm^{-1}. The measured spectrum also has the appearance of a Hund's case (b) $^2\Sigma-$Hund's case (a) $^2\Pi$ transition. Again, lower state combination differences were used to assign rotational quantum numbers to the lines in the spectrum, which belonged to the P_{12}, R_{12}, and Q_{22} branches.

For CaF it was found that in the previous work of Fowler[18] the vibrational bands of the $D^2\Sigma^+$ state had been misnumbered by one vibrational quantum number.[2,6] With this in mind, a search was initiated to investigate this same possibility for the $D^2\Sigma^+$ state of SrF. Again with the pump laser fixed to the Q_{12} and P_{11} band heads of the (0,0) $A^2\Pi_{1/2}-X^2\Sigma^+$ transition, a search was conducted by scanning the probe laser over the range 12670−12730 cm^{-1}, which corresponded to a decrease in probe laser frequency approximately equal to the vibrational energy spacing reported for the $D^2\Sigma^+$ state (∼552.1 cm^{-1}).[18] The two panels in Figure 3 show portions of the data obtained in the search region. The general appearance of the spectrum suggests a Hund's case (b) $^2\Sigma-$Hund's case (a) $^2\Pi$ transition. In the top panel, the high wavenumber side of the spectrum is shown. Using lower state combination differences, transitions arising from the Q_{11}, P_{21}, R_{11}, and Q_{21} branches were identified. The appearance of this spectrum is similar to that of the higher energy $D^2\Sigma^+-A^2\Pi_{1/2}$ transition where the Q_{11} and P_{21} branches also exhibit band heads. However, unlike in the higher energy transition the R_{11} and Q_{21} branches also exhibit band heads (12724 cm^{-1}). The presence of band heads in P, Q, and R branches is very unusual and suggests that this $^2\Sigma^+$ state is perturbed (the $A^2\Pi$ state is unperturbed). Further evidence for a perturbation in the $^2\Sigma^+$ state can be found in the lower panel of Figure 3, which shows the P_{11} branch. From 12690 to 12680.5 cm^{-1} the lines become more closely spaced, similar to the P_{11} branch of the previously observed higher energy $D^2\Sigma^+-A^2\Pi_{1/2}$ transition. However, unlike the P_{11} branch of the previously observed $D^2\Sigma^+-A^2\Pi_{1/2}$ transition, which exhibits a band head at low wavenumbers, the lines in the new $^2\Sigma^+-A^2\Pi_{1/2}$ transition begin to be spaced further apart from 12680.5 to 12670 cm^{-1}. Again, this pattern suggested that the new $^2\Sigma^+$ state was perturbed. To further investigate this new $^2\Sigma^+$ state, the pump laser was tuned to 15352 cm^{-1} and the Q_{22} and P_{21} band heads of the (0,0) $A^2\Pi_{3/2}-X^2\Sigma^+$ transition were excited. The probe laser was scanned from 12955 to 13010 cm^{-1} and the $^2\Sigma^+-A^2\Pi_{3/2}$ transition was observed. This transition exhibited the same general appearance of the $D^2\Sigma^+-A^2\Pi_{3/2}$ transition and was perturbed in a manner similar to the $^2\Sigma^+-A^2\Pi_{1/2}$ transition. Because this new $^2\Sigma^+$ state was found to lie lower in energy than the $D^2\Sigma^+$ state by an amount of energy almost identical to the vibrational spacing reported for the $D^2\Sigma^+$ state, the lower energy transition was tentatively labeled as the (0,0) $D^2\Sigma^+-A^2\Pi$ transition and the higher energy transition was labeled as the (1,0) $D^2\Sigma^+-A^2\Pi$ transition. A more detailed discussion of the evidence for this assignment is presented in the discussion section.

4. Analysis

A simultaneous least-squares fit of the data measured for the (0,0) $C^2\Pi-A^2\Pi$, (0,0) $D^2\Sigma^+-A^2\Pi$, and (1,0) $D^2\Sigma^+-A^2\Pi$ transitions to the appropriate effective molecular Hamiltonian was conducted. This Hamiltonian has the general form[41]

$$\hat{H}_{\text{eff}} = \hat{H}_{\text{rot}} + \hat{H}_{\text{SO}} + \hat{H}_{\Lambda\text{-doubling}} + \hat{H}_{\text{SR}} \qquad (1)$$

where $\hat{H}_{\text{rot}}$ describes the rotation of the molecule and centrifugal distortion to the rotation, $\hat{H}_{\text{SO}}$ describes the spin−orbit interaction in a $^2\Pi$ state, $\hat{H}_{\Lambda\text{-doubling}}$ describes the Λ-doubling interaction in a $^2\Pi$ state and $\hat{H}_{\text{SR}}$describes the spin-rotation interaction in a $^2\Sigma$ state. To minimize uncertainties in the lower state parameters, data obtained from the molecular beam study of the $A^2\Pi-X^2\Sigma^+$ transition[21] and millimeter-wave transitions[25] (corrected for unresolved hyperfine structure) measured for SrF were included in the final fit. In total, six pure rotational transitions of the $X^2\Sigma^+$ state, 131 lines from the (0,0) $A^2\Pi-X^2\Sigma^+$ transition, 221 lines from the (0,0) $C^2\Pi-A^2\Pi$ transition, 231 lines from the (0,0) $D^2\Sigma^+-A^2\Pi$ transition, and 74 lines from the (1,0) $D^2\Sigma^+-A^2\Pi$ transitions were included in the final fit. The data measured in this work (including those lines of the (0,0) $D^2\Sigma^+-A^2\Pi$ transition that were assigned but not included in the fit) are listed in Table S1 of the Supporting Information. In the fit, a weighting factor of 0.000003 cm^{-1} was used for the pure rotational transitions data, 0.003 cm^{-1} for the $A^2\Pi-X^2\Sigma^+$ transition and 0.005 cm^{-1} for the OODR data, in accordance with the respective experimental uncertainties.

Table 1 lists the spectroscopic parameters derived from the least-squares fit. The parameters for the $X^2\Sigma^+$ and $A^2\Pi$ states are in good agreement with those determined in the previous spectroscopic work.[21,25] For the $C^2\Pi$ state, the values of the band origin, T, the spin−orbit constant, A, and the rotational

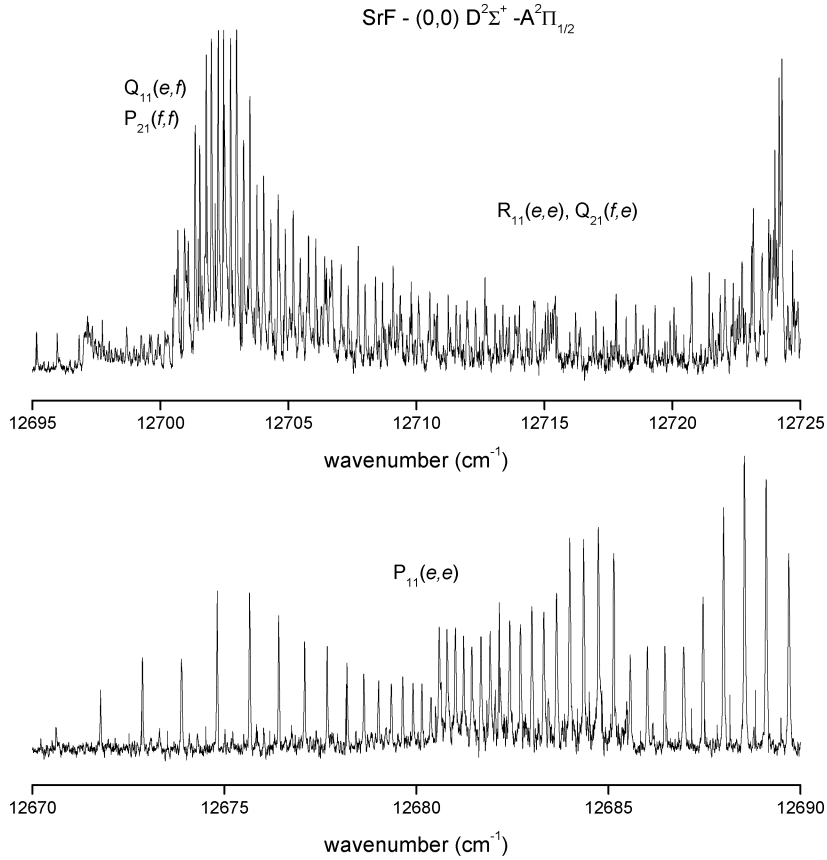

Figure 3. The spectrum of the (0,0) $D^2\Sigma^+-A^2\Pi_{1/2}$ transition. The high wavenumber side of the spectrum is shown in the top panel and the low wavenumber side is displayed in the bottom panel. The appearance of the spectrum resembles the pattern expected for a Hund's case (b) $^2\Sigma-$Hund's case (a) $^2\Pi$ transition. In the top panel the lines were assigned to the Q_{11}, P_{21}, R_{11}, and Q_{21} branches, all of which exhibit a band head. This atypical situation suggests that the $D^2\Sigma^+$ ($v = 0$) state is perturbed. In the bottom panel the lines of the P_{11} branch are shown. Initially the line spacing decreases from the high wavenumber side of the spectrum to the low wavenumber side, similar to (1,0) $D^2\Sigma^+-A^2\Pi_{1/2}$ transition. However, at ~12680.5 cm^{-1} the line spacing begins to increase again, further suggesting that the $D^2\Sigma^+(v = 0)$ state is perturbed.

TABLE 1: Spectroscopic Constants (in cm^{-1}) for SrF

constant[a]	$X^2\Sigma^+$	$A^2\Pi$	$C^2\Pi$	$D^2\Sigma^+$ ($v = 0$)	$D^2\Sigma^+$ ($v = 1$)
T	0.0	15216.34287(47)	27384.67113(93)	27773.8168(42)	28327.5784(12)
B	0.24975935(23)	0.2528335(37)	0.2462110(39)	0.263677(28)	0.2627533(42)
D	$2.4967(35) \times 10^{-7}$	$2.546(25) \times 10^{-7}$	$2.897(24) \times 10^{-7}$	$7.07(43) \times 10^{-7}$	$2.575(25) \times 10^{-7}$
γ	$2.4974(30) \times 10^{-3}$			−0.016666(82)	0.020367(63)
γ_D					$-2.963(39) \times 10^{-6}$
A		281.46138(52)	57.9048(14)		
A_D			$4.103(18) \times 10^{-4}$		
p		−0.133002(28)	$3.712(67) \times 10^{-3}$		
q			$-4.16(46) \times 10^{-5}$		

[a] Values in parentheses are 1σ standard deviations, in units of the last significant digits.

constant, B, are reasonably similar to the previous estimates of 27355.69 cm^{-1}, 61 cm^{-1}, and 0.24566 cm^{-1}, respectively.[36] The Λ-doubling parameters p and q have been determined for the first time. A value of q could be determined for the $C^2\Pi$ state, because of the high J values of the transitions observed.

Spectroscopic constants derived for the $D^2\Sigma^+(v = 1)$ state are also included in Table 1. The rotational, centrifugal distortion, and spin-rotation constants have been determined for the first time. The values of B and D are similar to those obtained for the $X^2\Sigma^+$ state; however, the value of the spin-rotation constant is about an order of magnitude larger. Due to the high J values included in the data set, it was necessary to include a centrifugal distortion constant to the spin rotation, γ_D, in the fit.

Fitting of the (0,0) $D^2\Sigma^+-A^2\Pi$ transition data was not as straightforward as it was for the other transitions due to the perturbation in the $D^2\Sigma^+$ ($v = 0$) state. Attempts to model all of the data recorded for this transition with eq 1 resulted in an extremely poor fit. On the basis of the location of the perturbation in the spectrum, only transitions with values of $J' \leq 22.5$ were included in the fit. The resulting spectroscopic constants are included in Table 1. The value of B is similar to that determined for the other states of SrF, in particular to that of the $D^2\Sigma^+$ ($v = 1$) state. However, the value of the centrifugal distortion constant, D, is more than two times as large than it is in the other states listed in Table 1. This suggests that D is acting as more of a fitting parameter and that the low J lines are still affected by the perturbation. A value of the spin rotation constant was also determined; however it was found to possess the opposite sign of the value of γ obtained for the $D^2\Sigma^+$ ($v = 1$) state.

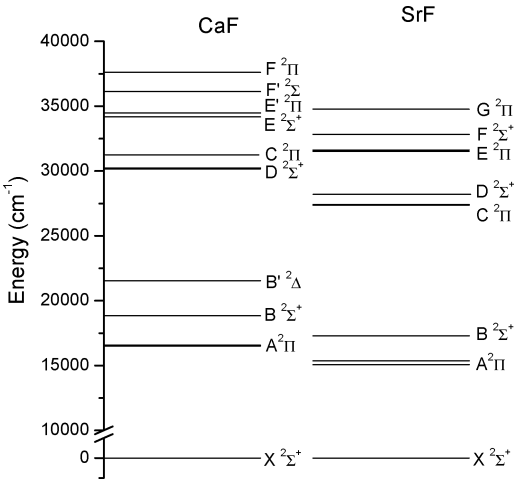

Figure 4. Energy level diagram of the observed electronic states of CaF and SrF below 40000 cm^{-1}. The electronic states of SrF are at lower energy relative to the corresponding states of CaF. In both molecules the $C^2\Pi$ and $D^2\Sigma^+$ states appear to be separated from the lower energy A and B states and higher energy E and F states.

5. Discussion

As mentioned previously, for CaF the lowest vibrational level observed for the $D^2\Sigma^+$ state by Fowler was assumed to be $v = 0$.[18] In a subsequent investigation, another $^2\Sigma^+$ state was identified at lower energy than the $D^2\Sigma^+$ state and labeled the $C'^2\Sigma^+$ state. However, the $C'^2\Sigma^+$ state was later identified as the $v = 0$ level of the $D^2\Sigma^+$ state, thereby increasing the numbering of the vibrational levels of the $D^2\Sigma^+$ state observed by Fowler by 1.[2,6] As a result, only one $^2\Sigma^+$ state was observed around 30000 cm^{-1}, which is supported by ab initio calculations.[42]

A similar mislabeling of the vibrational quantum numbers appears to exist for the $D^2\Sigma^+$ state of SrF. According to Fowler,[18] the $v = 0$ level of the $D^2\Sigma^+$ state has a term value of 28322.6 cm^{-1}, and in this work a $^2\Sigma^+$ state was observed at approximately this energy, 28327.5784 cm^{-1}. However, a second $^2\Sigma^+$ state was identified in this work at 27773.8168 cm^{-1}, which is 553.7616 cm^{-1} lower in energy than the previously labeled $D^2\Sigma^+$ ($v = 0$) state. The difference in energy between these two $^2\Sigma^+$ states is almost exactly equal to the value of ω_e reported by Fowler for the $D^2\Sigma^+$ state, 552.1 cm^{-1}. Despite the incorrect assignment of the vibrational quantum numbers in the $D^2\Sigma^+$ state of CaF, the value of ω_e reported by Fowler (650.7 cm^{-1}) was found to be almost identical to the value measured in a subsequent study (657.33 cm^{-1}). Therefore, the value of ω_e for the $D^2\Sigma^+$ of SrF is probably reliable and the energy difference between the two $^2\Sigma^+$ states suggests that the lower energy $^2\Sigma^+$ state is most likely the $v = 0$ level of the $D^2\Sigma^+$ state and not a new $^2\Sigma^+$ state.

Additional evidence for both $^2\Sigma^+$ states being different vibrational levels of the $D^2\Sigma^+$ state can be found by comparing the energy level diagrams of CaF and SrF, which are shown in Figure 4. In CaF the $C^2\Pi$ and $D^2\Sigma^+$ states are more than 10000 cm^{-1} higher in energy than the $A^2\Pi$ and $B^2\Sigma^+$ states and ~3000 cm^{-1} lower in energy than the next $^2\Sigma^+$ or $^2\Pi$ states. There is no other $^2\Sigma^+$ state located in this ~13000 cm^{-1} region. In the ligand field model of Rice, Field, and Martin[10] the electronic structure of the calcium monohalides was described as arising from a single unpaired valence electron localized around the metal cation of an M^+X^- molecule. This model was found to describe the low-lying states of CaF quite satisfactorily. The model was further extended to strontium monohalides by Allouche, Wannous, and Aubert-Frécon[12] with similar results. Therefore, it is not unreasonable to expect the electronic structure of SrF to be similar to that of CaF and in this case a second $^2\Sigma^+$ state would not be expected to be present in the energy region between the $A^2\Pi$ and $B^2\Sigma^+$ states and the E state in SrF.

An examination of the rotational constants obtained for each $^2\Sigma^+$ state determined in this study also suggests that they are different vibrational levels of the same electronic state. The value of the rotational constant in the lower energy $^2\Sigma^+$ state ($D^2\Sigma^+$ $v = 0$) is 0.263677 cm^{-1} and in the higher energy $^2\Sigma^+$ state ($D^2\Sigma^+$ $v = 1$) it is 0.2627533 cm^{-1}, both of which are quite similar. If both $^2\Sigma^+$ states are considered to be vibrational levels of the $D^2\Sigma^+$ state, then the value of α_e, the vibration−rotation constant, is calculated to be 9.24×10^{-4} cm^{-1} ($B_e = 0.264139$ cm^{-1}). For the $X^2\Sigma^+$ state of SrF, $\omega_e = 501$ cm^{-1} [29] and $\alpha_e = 1.551101 \times 10^{-3}$ cm^{-1}, both of which are similar to the $D^2\Sigma^+$ state values.[29] Therefore, the rotational constants of the two $^2\Sigma^+$ states observed in this study are consistent with the assignment of the two $^2\Sigma^+$ states as different vibrational levels of the same electronic state. On the basis of the evidence provided, we feel confident that both $^2\Sigma^+$ states are different vibrational states of the $D^2\Sigma^+$ state. Therefore, in the work of Fowler, the vibrational quantum numbers of the $D^2\Sigma^+$ state should be increased by 1. In our study, the lower energy $^2\Sigma^+$ state is therefore labeled as the ($D^2\Sigma^+$ $v = 0$) level and the higher energy $^2\Sigma^+$ state is labeled as the ($D^2\Sigma^+$ $v = 1$) level. It must be mentioned that this work does not completely rule out the possibility that the actual $v = 0$ level may lie still lower in energy.

Clear evidence for a perturbation in the measured spectrum of the (0,0) $D^2\Sigma^+ - A^2\Pi_{1/2}$ transition is shown in Figure 3. The bottom panel of this figure shows the P_{11} branch. In this spectrum the lines initially become more closely spaced from the high wavenumber side to the low wavenumber side. This is similar to the P_{11} branch of the (1,0) $D^2\Sigma^+ - A^2\Pi_{1/2}$ transition, which is shown in the Figure 2. However, unlike the P_{11} branch of the (1,0) $D^2\Sigma^+ - A^2\Pi_{1/2}$ transition, which terminates on the low wavenumber side with a band head, the spacing of the lines of the P_{11} branch of the (0,0) $D^2\Sigma^+ - A^2\Pi_{1/2}$ transition begins to increase below 12680.5 cm^{-1}. Because the $A^2\Pi$ state is unperturbed, this suggests that there is a perturbation in the $D^2\Sigma^+$ ($v = 0$) state localized at about $J = 22.5$. Further evidence for the perturbation can be found by examining the upper panel of Figure 3. In this portion of the spectrum the Q_{11} and P_{21} branches exhibit band heads at 12697.5 cm^{-1}. These branches also exhibit band heads in the (1,0) $D^2\Sigma^+ - A^2\Pi_{1/2}$ transition at 13249 cm^{-1}. However, the R_{11} and Q_{21} branches also exhibit band heads in the (0,0) $D^2\Sigma^+ - A^2\Pi_{1/2}$ transition (12724 cm^{-1}) while they do not in the (1,0) $D^2\Sigma^+ - A^2\Pi_{1/2}$ transition. The presence of band heads in the P, R, and Q branches of the same transition is further evidence for a perturbation in the $D^2\Sigma^+$ ($v = 0$) state. While the exact nature of the perturbation could not be ascertained in this study, the energy level diagram of SrF, shown in Figure 4 can be used to suggest a possible perturbing state. For SrF the $C^2\Pi$ ($v = 0$) state is found to lie 389 cm^{-1} lower in energy than the $D^2\Sigma^+$ $v = 0$ level. The value of ω_e for the $C^2\Pi$ state has been reported[35] to be 454.2245 cm^{-1}. Taking into account the spin−orbit splitting of the $C^2\Pi$ ($v = 0$) state, the $C^2\Pi_{1/2}(v = 1)$ level is calculated to lie at ~27810 cm^{-1} and the $C^2\Pi_{3/2}(v = 1)$ level is located at ~27868 cm^{-1}. These states are within 36 and 94 cm^{-1}, respectively, of the $D^2\Sigma^+$ ($v = 0$) state. Because of their close proximity, these states are most likely the cause of the perturbation observed in the $D^2\Sigma^+$ ($v = 0$) state. Additional lines were observed in the spectra of the

TABLE 2: Spin−Orbit Constants (in cm^{-1}) of CaF, SrF, and SrOH

constant[a]	CaF	SrF[d]	SrOH[e]
$A^2\Pi$	71.491(42)[b]	281.46138(52)	263.58783(64)
$C^2\Pi$	29.320(4)[c]	57.9048(14)	24.6607(12)

[a] Values in parentheses are 1σ standard deviations, in units of the last significant digits. [b] From ref 1. [c] From ref 2. [d] This work. [e] From ref 37.

TABLE 3: Bond Lengths (in Å) of CaF and SrF

constant	$X^2\Sigma^+$	$A^2\Pi$	$C^2\Pi$	$D^2\Sigma^+$
CaF[a]	1.955	1.940	2.012	1.893
SrF[b]	2.079	2.066	2.094	2.023

[a] Calculated using the rotational constants of refs 1 and.2 [b] Calculated using the rotational constants from this work.

(1,0) $D^2\Sigma^+-A^2\Pi_{1/2}$ and (1,0) $D^2\Sigma^+-A^2\Pi_{3/2}$ transitions that could not be assigned and were only observed on the higher wavenumber side of each spectrum. Unfortunately, there were not enough lines to make assignments. The difference in the vibrational spacing of the $C^2\Pi$ state (454.2245 cm^{-1}) and the $D^2\Sigma^+$ ($v = 0$) state (553.8 cm^{-1}) allows for the $D^2\Sigma^+$ ($v = 1$) state to not be perturbed significantly by the $C^2\Pi$ ($v = 2$) level. As a result the (1,0) $D^2\Sigma^+-A^2\Pi_{1/2}$ and (1,0) $D^2\Sigma^+-A^2\Pi_{3/2}$ transitions do not appear to exhibit any significant perturbations.

For SrF, CaF, and SrOH there now exists a rotational analysis for the $C^2\Pi$ and $D^2\Sigma^+$ states of each molecule. As a result the spectroscopic parameters in these states can be compared. Table 2 lists the spin−orbit constants of the $A^2\Pi$ and $C^2\Pi$ states for each molecule. For all three molecules the spin−orbit constants of the $C^2\Pi$ state are found to be significantly smaller than those of the $A^2\Pi$ state. For CaF and SrOH this trend was rationalized in terms of a change in the atomic orbital character of the unpaired electron between the two states.[10,37] From the ligand field model,[10] the atomic orbital character of the $A^2\Pi$ state of CaF was calculated to be 69% 4p, 24% 3d, and 7% higher energy orbitals. In the $C^2\Pi$ state of CaF the atomic orbital character was calculated to be 4% 4p, 26% 3d, and 70% higher energy orbitals. In the $C^2\Pi$ state the unpaired electron is in an orbital that is mostly higher energy atomic orbital in character and these orbitals have lower atomic spin orbit constants ($\zeta_{4p} = 148$ cm^{-1} vs $\zeta_{3d} = 25$ cm^{-1}).[10] As a result the molecular spin−orbit parameter of the molecule is reduced in the $C^2\Pi$ state. This rationale was applied to explain the decrease in spin−orbit constant in the $C^2\Pi$ state of SrOH relative to the $A^2\Pi$ state. Although no theoretical calculations of the orbital character of the $C^2\Pi$ state of SrF have been reported, the decrease in the spin−orbit constant of the $C^2\Pi$ state relative to the $A^2\Pi$ state suggests a similar change in atomic orbital character. Additional theoretical work is warranted to investigate the atomic orbital character of the unpaired electron in this state of SrF.

Table 3 lists the metal fluoride bond lengths of SrF and CaF in the $X^2\Sigma^+$, $A^2\Pi$, $C^2\Pi$, and $D^2\Sigma^+$ states. The SrF bond lengths follow the same general trend exhibited by the CaF bond lengths with the $C^2\Pi$ and $D^2\Sigma^+$ states representing extremes. Of the states listed the metal−fluoride bond length is the longest for both molecules in the $C^2\Pi$ state. For CaF a large dipole moment was measured in the $C^2\Pi$ (9.24 D) state as compared to the $A^2\Pi$ (2.45D) state.[5] The increase in the dipole moment was explained by a polarization of the orbital containing the unpaired electron in the direction of the negatively charged ligand.[5] The resulting increased electrostatic repulsion would also lengthen the metal−fluoride bond length. Although dipole measurements of SrF in its $C^2\Pi$ state do not exist, the metal−fluoride bond length in the $C^2\Pi$ state suggests the same scenario. In the $D^2\Sigma^+$ state the metal−fluoride bond length is the shortest in SrF and in CaF. This result suggests that the unpaired electron in the $D^2\Sigma^+$ state of both CaF and SrF has a similar atomic orbital character (nominally 6s for the Sr case).[9]

The $A^2\Pi$ and $B^2\Sigma^+$ states of SrF are a good example of a pair of unique perturbing states.[20] Evidence for this conclusion arises from the nearly identical values of the Λ-doubling constant, p, in the $A^2\Pi$ state (−0.130 cm^{-1})[21] and the spin-rotation constant, γ, in the $B^2\Sigma^+$ state (−0.134 cm^{-1}).[20] According to the pure precession approximation the Λ-doubling parameters, p and q of a $^2\Pi$ state can be calculated using the following expressions[43]

$$p = \frac{2A_\Pi B_\Pi l(l+1)}{T_\Pi - T_\Sigma} \quad (2)$$

and

$$q = \frac{2B_\Pi{}^2 l(l+1)}{T_\Pi - T_\Sigma} \quad (3)$$

and the spin-rotation parameter, γ, is given by the expression[43]

$$\gamma = \frac{2A_\Pi B_\Sigma l(l+1)}{T_\Pi - T_\Sigma} \quad (4)$$

In eqs 2−4, l represents the effective angular momentum of the unpaired electron. For the $A^2\Pi$ and $B^2\Sigma^+$ states of SrF when a value of $l = 1$ is substituted into eqs 2 and 4, p and γ are calculated to be −0.130 cm^{-1}, which is in excellent agreement with the experimental values. The observed p and γ values of the $C^2\Pi$ and $D^2\Sigma^+$ of SrF allow for an examination of the unique perturber/pure precession behavior for these two states. The value of p in the $C^2\Pi$ state is 3.712×10^{-3} cm^{-1} and the value of γ in the $D^2\Sigma^+$ ($v = 0$) state is −0.016666 cm^{-1}. These values differ in sign and by an order of magnitude, suggesting that the $C^2\Pi$ and $D^2\Sigma^+$ states do not form a unique perturber pair. For CaF, the value of p in the $C^2\Pi$ state is 1.1×10^{-3} cm^{-1} and the value of γ in the $D^2\Sigma^+$ state is 0.3×10^{-3} cm^{-1} [2]. The similarity of these values suggests that the $C^2\Pi$ and $D^2\Sigma^+$ states of CaF form a unique perturbing pair. The sign of p and γ for CaF in these states is also in agreement with the pure precession relations for these parameters. Previously, it was suggested that the atomic orbital character of the unpaired electron in the $C^2\Pi$ state was similar in both CaF and SrF and that this was also the case for the $D^2\Sigma^+$ states. Therefore, the failure of the $C^2\Pi$ and $D^2\Sigma^+$ states in SrF to form a unique perturbing pair is somewhat surprising. This result may be due to the perturbation in the $D^2\Sigma^+$ ($v = 0$) state affecting the values of γ and p. The difference in the values of γ in the $D^2\Sigma^+$ ($v = 0$) and $D^2\Sigma^+$ ($v = 1$) states is consistent with this observation. It would be useful to obtain additional data to definitively identify the perturbing state and subsequently conduct a deperturbation analysis on all of these data.

Acknowledgment. Financial support for this work was provided by the Natural Science and Engineering Research Council (NSERC) of Canada. Some support was also provided by the UK Engineering and Physical Sciences Research Council (EPSRC).

Supporting Information Available: Transition data for SrF. This material is available free of charge via the Internet at http://pubs.acs.org.

References and Notes

(1) Kaledin, L. A.; Bloch, J. C.; McCarthy, M. C.; Field, R. W. *J. Mol. Spectrosc.* **1999**, *197*, 289.
(2) Gittins, C. M.; Harris, N. A.; Field, R. W.; Vergès, J.; Effantin, C.; Bernard, A.; d'Incan, J.; Ernst, W. E.; Bundgen, P.; Engels, B. *J. Mol. Spectrosc.* **1993**, *161*, 303.
(3) Anderson, M. A.; Allen, M. D.; Ziurys, L. M. *Astrophys. J.* **1994**, 424–503.
(4) Charron, F.; Guo, B.; Zhang, K.-Q.; Morbi, Z.; Bernath, P. F. *J. Mol. Spectrosc.* **1995**, *171*, 160.
(5) Ernst, W. E.; Kändler, J. *Phys. Rev. A* **1989**, *39*, 1575.
(6) Vergès, J.; Effantin, C.; Bernard, A.; Topouzkhanian, A.; Allouche, A. R.; d'Incan, J.; Barrow, R. F. *J. Phys. B* **1993**, *26*, 279.
(7) Bernath, P. F.; Field, R. W. *J. Mol. Spectrosc.* **1980**, *82*, 339.
(8) Harris, N. A.; Field, R. W. *J. Chem. Phys.* **1993**, *98*, 2642.
(9) Berg, J. M.; Murphy, J. E.; Harris, N. A.; Field, R. W. *Phys. Rev. A* **1993**, *48*, 3012.
(10) Rice, S. F.; Martin, H.; Field, R. W. *J. Chem. Phys.* **1985**, *82*, 5023.
(11) Mestdagh, J. M.; Visticot, J. P. *Chem. Phys.* **1991**, *155*, 79.
(12) Allouche, A. R.; Wannous, G.; Aubert-Frécon, M. *Chem. Phys.* **1993**, *170*, 11.
(13) Altunata, S. N.; Coy, S. L.; Field, R. W. *J. Chem. Phys.* **2005**, *123*, 084319.
(14) Arif, M.; Jungen, Ch.; Roche, A. L. *J. Chem. Phys.* **1997**, *106*, 4102.
(15) DeMille, D.; Cahn, S. B.; Murphee, D.; Rahmlow, D. A.; Kozlov, M. G. *Phys. Rev. Lett.* **2008**, *100*, 023003.
(16) Johnson, R. C. *Proc. R. Soc. London, Ser. A* **1929**, 122–161.
(17) Harvey, A. *Proc. R. Soc. London, Ser. A* **1931**, *133*, 336.
(18) Fowler, C. A. *Phys. Rev.* **1941**, *59*, 645.
(19) Steimle, T. C.; Domaille, P. J.; Harris, D. O. *J. Mol. Spectrosc.* **1978**, *73*, 441.
(20) Steimle, T. C.; Domaille, P. J.; Harris, D. O. *J. Mol. Spectrosc.* **1977**, *68*, 134.
(21) Steimle, T. C.; Fletcher, D. A.; Scurlock, C. T. *J. Mol. Spectrosc.* **1993**, *158*, 487.
(22) Brown, J. M.; Milton, D. J.; Steimle, T. C. *Faraday Discuss.* **1981**, *71*, 151.
(23) Ernst, W. E.; Schroder, J. O. *Chem. Phys.* **1983**, *78*, 363.
(24) Domaille, P. J.; Steimle, T. C.; Harris, D. O. *J. Mol. Spectrosc.* **1977**, *68*, 146.
(25) Schutze-Pahlmann, H.-U.; Ryzlewicz, Ch.; Hoeft, J.; Törring, T. *Chem. Phys. Lett.* **1982**, *93*, 74.
(26) Childs, W. J.; Goodman, L. S.; Renhorn, I. *J. Mol. Spectrosc.* **1981**, *87*, 522.
(27) Ernst, W. E. *Appl. Phys. B: Laser Opt.* **1983**, *30*, 105.
(28) Azuma, Y.; Childs, W. J.; Goodman, G. L.; Steimle, T. C. *J. Chem. Phys.* **1990**, *93*, 5533.
(29) Colarusso, P.; Guo, B.; Zhang, K.-Q.; Bernath, P. F. *J. Mol. Spectrosc.* **1996**, *175*, 158.
(30) Ernst, W. E.; Kändler, J.; Kindt, S.; Törring, T. *Chem. Phys. Lett.* **1985**, *113*, 351.
(31) Kändler, J.; Martell, T.; Ernst, W. E. *Chem. Phys. Lett.* **1989**, *155*, 470.
(32) Barrow, R. F.; Beale, J. R. *Chem. Commun.* **1967**, *12*, 606.
(33) Nitsch, C.; Schroder, J. O.; Ernst, W. E. *Chem. Phys. Lett.* **1988**, *148*, 130.
(34) Novikov, M. M.; Gurvich, L. V. *Opt. Spectrosc.* **1967**, *22*, 395.
(35) Ram, R. S.; Rai, S. B.; Upadhya, K. N. *Pramana* **1980**, *15*, 413.
(36) Rao, V. M.; Rao, M. L. P.; Narayana, A. L. *Opt. Pura Apl.* **1982**, *15*, 99.
(37) Wang, J.-G.; Sheridan, P. M.; Dick, M. J.; Bernath, P. F. *J. Mol. Spectrosc.* **2005**, *236*, 21.
(38) Wang, J.-G.; Dick, M. J.; Sheridan, P. M.; Yu, S.; Bernath, P. F. *J. Mol. Spectrosc.* **2007**, *245*, 26.
(39) Yu, S.; Wang, J.-G.; Sheridan, P. M.; Dick, M. J.; Bernath, P. F. *J. Mol. Spectrosc.* **2006**, *240*, 26.
(40) Dick, M. J.; Sheridan, P. M.; Wang, J.-G.; Yu, S.; Bernath, P. F. *J. Mol. Spectrosc.* **2006**, *240*, 238.
(41) Brown, J. M.; Colbourn, E. A.; Watson, J. K. G.; Wayne, F. D. *J. Mol. Spectrosc.* **1979**, *74*, 294.
(42) Bündgen, P.; Engels, B.; Peyerimhoff, S. D. *Chem. Phys. Lett.* **1991**, *176*, 407.
(43) Lefebvre-Brion, H.; Field, R. W. *The Spectra and Dynamics of Diatomic Molecules*; Elesevier: Amsterdam, The Netherlands, 2004.

JP9020855